Original Article

THREE-DIMENSIONAL FINITE ELEMENT ANALYSIS OF FORCES PRODUCED BY DIFFERENT ORTHODONTIC ARCHWIRES

*Minaz Mubeen[1], Rohan Mascarenhas[1], Jemshid Ahamed Achoth[1], Dilshad Umar[1]**

[1]*Department of Orthodontics and Dentofacial Orthopedics, Yenepoya Dental College, Yenepoya (Deemed to be University), Mangalore, Karnataka, India. orthodil@gmail.com*

Received: 28 January 2026; **Revised:** 29 March 2026; **Accepted:** 06 April 2026 https://doi.org/10.51847/5TJsgAZyU2

ABSTRACT

The biomechanical properties of orthodontic archwires influence the efficacy and biological response of tooth movement. Austenitic (A-NiTi) and Martensitic (M-NiTi) nickel-titanium wires are widely used in clinical practice, yet their mechanical behavior under varying displacements remains quantified. Finite element analysis (FEA) offers a tool to simulate and evaluate such differences under conditions. To compare the force delivery, stress-strain distribution in the periodontal ligament (PDL), and dentoalveolar deformation induced by A-NiTi and M-NiTi archwires using a three-dimensional finite element model. A CBCT-derived model of a mandibular central incisor with its supporting structures was developed using MIMICS and CATIA software. A standard bracket-archwire system was modeled, incorporating 0.016-inch A-NiTi and M-NiTi wires. Displacements ranging from 0.5 mm to 2 mm were simulated in six directions (extrusive, intrusive, inward, outward, rotational, and angular). Forces generated by the wires were computed, and these were applied to the tooth model in ANSYS Workbench 15.0 to analyze stress-strain responses and deformation . A-NiTi wires exhibited higher force output and induced greater PDL stress and tooth deformation across all displacement types. Inward and outward displacements resulted in the highest mechanical responses. M-NiTi wires delivered lighter, more uniform forces, generating stress and strain , particularly favorable in multi-directional or rotational movements. The biomechanical performance of A-NiTi and M-NiTi wires varies significantly with displacement direction and magnitude. A-NiTi wires may be advantageous for rapid alignment, while M-NiTi offers gentler force profiles suited for biologically sensitive cases. Finite element modeling provides critical insights for optimizing wire selection in clinical orthodontics.

Key words: Finite element analysis, Nickel-Titanium, Orthodontics, Biomechanics, Periodontal ligament.

Introduction

Orthodontic tooth movement is a complex biological process initiated by mechanical forces that induce remodeling of the periodontal ligament (PDL) and alveolar bone. The efficacy of these forces depends on their magnitude, direction, and duration, which must be optimized to prevent tissue damage while ensuring efficient tooth displacement [1]. Nickel-titanium (NiTi) arch wires are widely used in orthodontics due to their unique properties, such as super elasticity and shape memory, which enable the delivery of continuous, light forces ideal for the initial alignment phase [1-5]. However, the biomechanical behavior of NiTi wires, particularly the differences between austenitic (A-NiTi) and martensitic (M-NiTi) phases, and their effects on the periodontium remain incompletely understood [6].

Finite element analysis (FEA) has emerged as a powerful tool to simulate orthodontic force systems and their biological impacts. Unlike traditional experimental methods, FEA allows for precise quantification of stress-strain distributions in the PDL and surrounding structures under controlled conditions [7-11]. Previous studies have highlighted the influence of wire composition and geometry on force delivery, but few have compared the biomechanical effects of A-NiTi and M-NiTi arch wires during multi-directional tooth movement [12, 13].

This study employs a three-dimensional finite element model to evaluate the forces generated by 0.016-inch A-NiTi and M-NiTi arch wires during displacement in six directions (intrusion, extrusion, inward, outward, rotation, and angulation). Additionally, it analyzes the resulting stress-strain patterns in the PDL and deformation of the tooth and alveolar bone. By simulating clinical scenarios, this research aims to provide insights into wire selection and optimizing force systems for efficient and biologically safe orthodontic treatment. The findings could enhance clinical decision-making, particularly in cases requiring complex tooth movements.

Materials and Methods

This study employed a three-dimensional finite element method (FEM) to quantitatively evaluate and compare the biomechanical behavior of two commercially available 0.016-inch nickel-titanium (NiTi) orthodontic arch wires, Austenitic NiTi (A-NiTi) and Martensitic NiTi (M-NiTi), under simulated clinical displacement conditions. The core objectives were to measure the forces generated by each wire type, analyze the resultant stress-strain distribution in the periodontal ligament (PDL), and assess the deformation patterns of the tooth and supporting alveolar bone [14-19].

Data acquisition and geometric modeling

A cone-beam computed tomography (CBCT) scan of the mandibular anterior region, inclusive of the central incisor and surrounding dentoalveolar structures, was acquired. Ethical approval was secured prior to patient data usage. The digital imaging data in DICOM format were imported into MIMICS (version 14.0, Materialize NV, Belgium), a medical image processing software, to perform segmentation and construct three-dimensional surface models of the tooth, PDL, cortical bone, and cancellous bone.

The segmented anatomical structures were exported in stereolithographic (STL) format and further processed in CATIA V5 R19 (Dassault Systèmes, France), a CAD software environment. Surface irregularities were rectified through model healing and meshing refinement to enhance anatomical accuracy. The bracket and arch wire assemblies were modeled independently using CAD tools and later integrated with the tooth geometry. A standard slot bracket was scanned using a blue light scanner and reproduced in the model. The arch wire was designed to span three teeth, engaged between the brackets of two lower central incisors, to replicate typical clinical alignment scenarios.

Material properties and meshing

All components in the finite element model were assigned linear elastic, isotropic material properties based on values reported in the literature. The Young's modulus and Poisson's ratio for each component were defined as follows: enamel (84 GPa, 0.3), dentin (18.6 GPa, 0.31), cortical bone (13.7 GPa, 0.3), cancellous bone (1.37 GPa, 0.3), PDL (0.07 MPa, 0.45), and stainless steel bracket (200 GPa, 0.3) **(Table 1)**.

Table 1. Material Properties Assigned to Finite Element Components

Component	Young's Modulus (GPa)	Poisson's Ratio	Remarks
Enamel	84	0.3	High stiffness
Dentin	18.6	0.31	Intermediate stiffness
Cortical Bone	13.7	0.3	Dense outer layer
Cancellous Bone	1.37	0.3	Spongy internal bone
Periodontal Ligament	0.07 (MPa)	0.45	Highly deformable
A-NiTi Wire	41–70	0.3	Superelastic
M-NiTi Wire	28–40	0.3	Thermally activated
Stainless Steel Bracket	200	0.3	Used in the bracket slot

The NiTi arch wires were modeled with distinct mechanical characteristics: A-NiTi was considered super elastic, while M-NiTi was treated as thermally activated with shape memory properties. These were incorporated through user-defined material models in the ANSYS Workbench 15.0 environment.

The entire assembly, consisting of the tooth, PDL, alveolar bone, bracket, and wire, was discretized using tetrahedral elements. A convergence test was conducted to ensure mesh density adequacy. The final model comprised approximately 300,000 nodes and 220,000 elements. Special emphasis was placed on mesh refinement at the PDL and root interface to ensure accurate stress resolution in this biologically critical zone **(Figure 1)**.

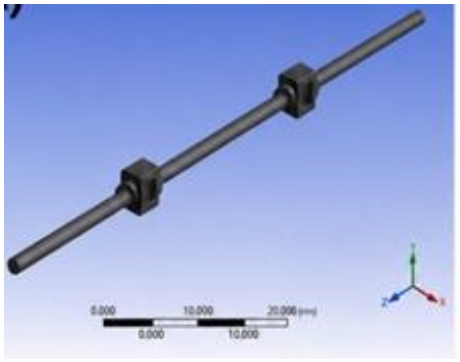

a)

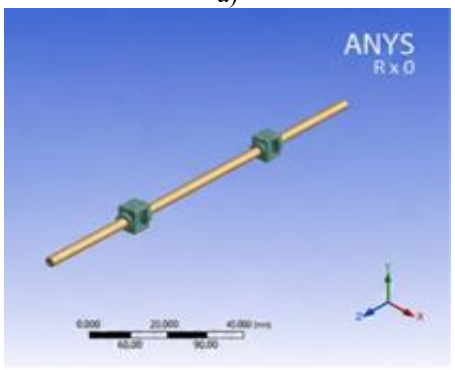

b)

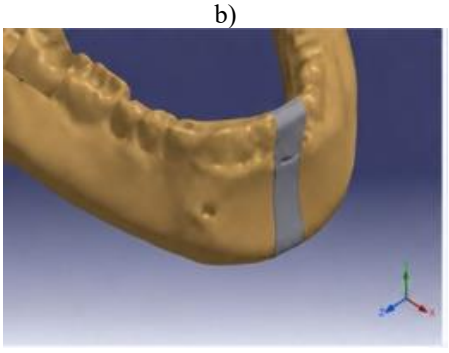

c)

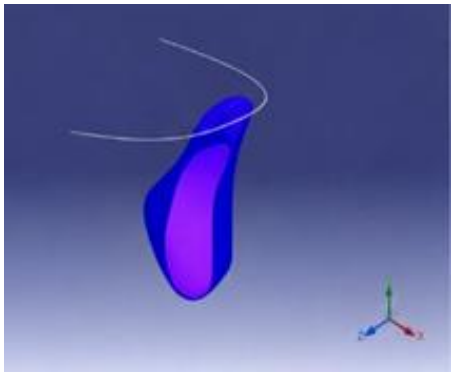

d)

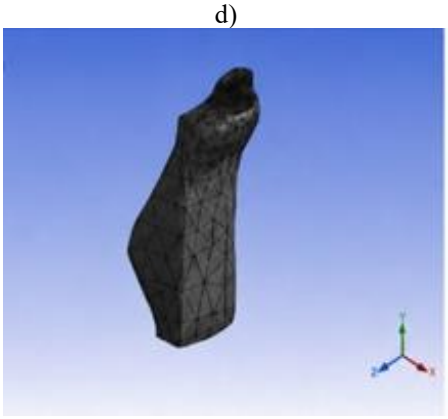

e)

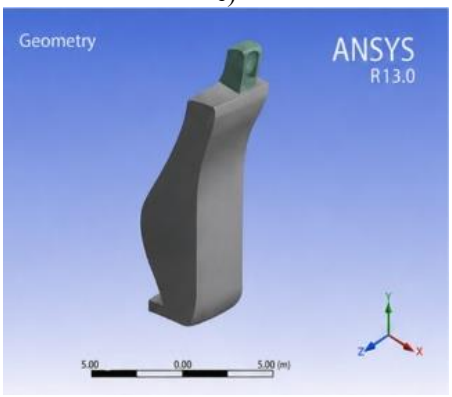

f)

Figure 1. Finite Element Model and Meshing. (a) Archwire–bracket assembly modeled in ANSYS. (b) Meshed archwire–bracket assembly used for force simulation. (c) CBCT-derived mandibular anterior segment. (d) Three-dimensional model of the mandibular central incisor with surrounding periodontal ligament. (e) Finite element mesh of the tooth model. (f) Final solid model of the mandibular central incisor used for biomechanical analysis.

Boundary conditions and loading protocol

Two sequential analyses were conducted: the wire deformation study and the biomechanical tooth response analysis.

In the first phase, the arch wire was analyzed in isolation. Boundary conditions were applied to simulate engagement within two bracket slots. The length of the wire spanned three teeth, with the central segment undergoing displacement in six clinical directions: extrusive, intrusive, inward (lingual), outward (labial), rotational, and angular. Displacements of 0.5 mm to 2 mm were applied incrementally. A coefficient of friction ($\mu = 0.28$) was defined between the arch wire and bracket to enable realistic sliding behavior. No constraints were placed on the wire ends, allowing free sliding within the bracket slots.

In the second phase, the quantified displacement forces from the first analysis were applied to the tooth model in corresponding directions. Boundary conditions were set by fixing the base of the alveolar bone to simulate physiological constraints. The contact between the archwire and the bracket/tooth was modeled as bonded to simplify computational requirements in the deformation analysis [20-29].

Finite element analysis procedure

The finite element simulations were performed using ANSYS Workbench 15.0. A two-step solver approach was utilized, comprising static structural analysis for both the wire deformation and the tooth-PDL-bone system. For the first analysis, reaction forces generated due to specific arch wire displacements were recorded. These were subsequently applied as input loads in the second analysis phase on the tooth model.

Stress and strain distributions within the PDL were assessed for each movement direction and for varying displacement magnitudes. Von Mises stress, principal stress values, and maximum shear stress were calculated. Similarly, displacement vectors were recorded to assess tooth and alveolar bone deformation. Additional simulations were performed to evaluate combined displacements (e.g., simultaneous extrusive and rotational forces) to reflect clinical multi-vectorial movement scenarios.

Validation and reproducibility

The modeled material properties and boundary conditions were cross-validated with published orthodontic and biomechanical literature. The geometric fidelity of the tooth model was corroborated through visual comparison with clinical CBCT slices and morphological anatomical references. To ensure consistency, all simulations were repeated thrice and analyzed for variation in peak stress values; results varied within a 5% margin, confirming computational reliability.

Results and Discussion

The results revealed significant differences in the force magnitudes produced by each wire under varied displacements, as well as in the resultant stress-strain responses within the periodontal ligament (PDL) and associated deformation patterns of the tooth and alveolar bone **(Table 2)**.

Table 2. Force Output of A-NiTi and M-NiTi Archwires by Direction and Displacement

Direction	Displacement (mm)	Force (A-NiTi, cN)	Force (M-NiTi, cN)
Extrusive	0.5	22.1	17.6
Extrusive	1.0	45.6	35.2
Extrusive	1.5	66.7	51.0
Extrusive	2.0	88.3	65.8
Inward	2.0	134.6	102.3
Outward	2.0	138.2	107.8
Rotational	2.0	26.7	20.4
Angular	2.0	24.5	19.1

In the first phase of the study, involving the isolated wire model, the A-NiTi arch wire consistently exhibited greater force output across all directions and magnitudes of displacement when compared to the M-NiTi wire. Force levels increased linearly with each incremental displacement, and this pattern was evident in both wires. **Figure 2** shows the deformation behavior of the NiTi arch wires under varied directional loads. However, the magnitude of forces recorded in the A-NiTi model was markedly higher, reflecting the higher elastic modulus and superelastic properties inherent to the Austenitic phase.

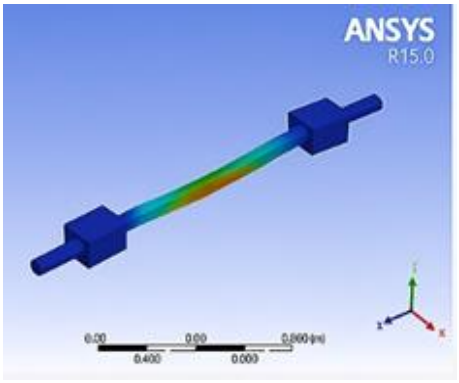

a)

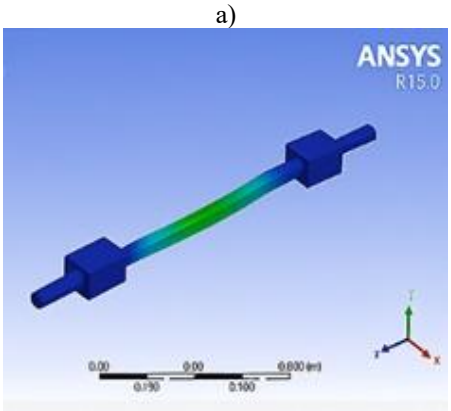

b)

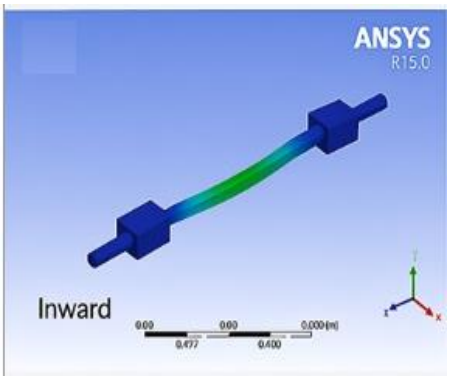

c)

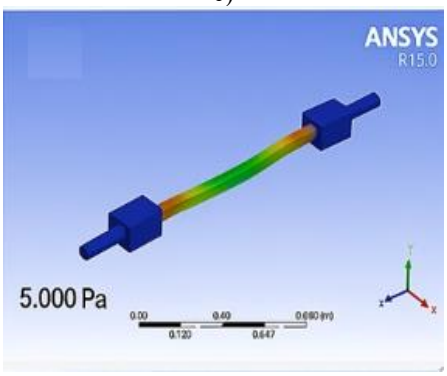

d)

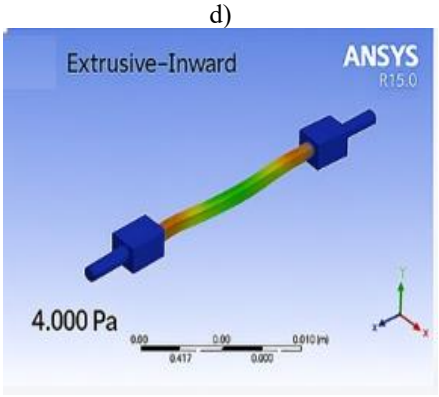

e)

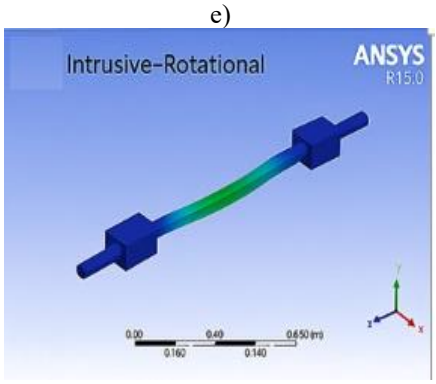

f)

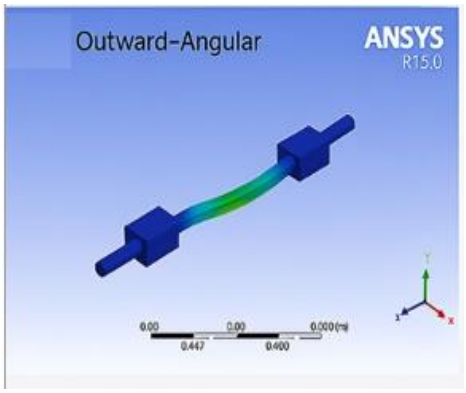

g)

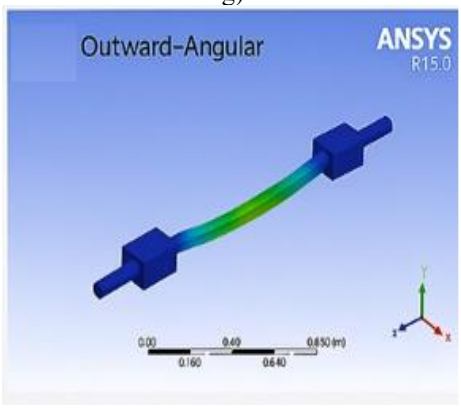

h)

Figure 2. Deformation Patterns Under Orthodontic Loading. The figure illustrates the deformation patterns of a 0.016-inch NiTi arch wire under eight distinct directional orthodontic forces, as simulated using ANSYS R15.0. Each subfigure represents a specific type of displacement, with color contours indicating total deformation or von Mises stress, ranging from blue (minimal) to red (maximal). Subfigure (a) shows deformation under an extrusive force, while (b) represents an intrusive displacement. Inward and outward force applications are depicted in (c) and (d), respectively. Combined extrusive-inward movement is illustrated in (e), and an intrusive-rotational force in (f). Angular displacements in an outward direction are demonstrated in (g) and (h), reflecting variations in directional load combinations.

Among the six directions of displacement analyzed, extrusive, intrusive, inward (lingual), outward (labial), rotational, and angular, the inward and outward movements elicited the highest force levels from both arch wire types. For instance, at a 2 mm displacement, the A-NiTi arch wire generated a peak force of 138.2 cN in the outward direction and 134.6 cN in the inward direction. By contrast, the M-NiTi wire demonstrated significantly lower force values for the same displacements, recording 107.8 cN and 102.3 cN, respectively **(Table 3)**. These findings suggest that labiolingual deflections result in nearly double the force output compared to vertical (intrusive/extrusive) or rotational displacements, irrespective of the wire type.

Table 3. Maximum PDL Stress and Strain (2 mm Displacement)

Direction	Wire Type	Max PDL Stress (MPa)	Max PDL Strain (%)
Extrusive	A-NiTi	0.027	7.4
Extrusive	M-NiTi	0.022	5.8
Inward	A-NiTi	0.038	10.2
Inward	M-NiTi	0.028	7.6
Outward	A-NiTi	0.036	9.8
Outward	M-NiTi	0.027	7.4
Rotational	A-NiTi	0.015	4.2
Rotational	M-NiTi	0.010	3.1

Extrusive and intrusive displacements were associated with moderate force magnitudes. In the extrusive direction, A-NiTi delivered forces ranging from 22.1 cN to 88.3 cN across the 0.5 mm to 2 mm displacement spectrum. In contrast, M-NiTi produced slightly lower values, ranging from 17.6 cN to 65.8 cN. Intrusive forces followed a similar trend, with A-NiTi generating between 20.3 cN and 83.4 cN, and M-NiTi producing 15.2 cN to 62.0 cN. These results reflect the stiffness differential between the two materials and underscore the relatively greater force capability of the superelastic A-NiTi variant.

Rotational and angular displacements yielded the lowest force outputs in both arch wire types. A-NiTi recorded forces ranging from 8.6 cN to 26.7 cN, while M-NiTi generated values between 6.9 cN and 20.4 cN across the displacement range. This reduction in force magnitude for rotational and angular movements is attributable to the geometric configuration of displacement and the limited structural resistance offered by the arch wire in those planes.

The second part of the analysis, involving the application of these displacement-derived forces to a fully modeled dentoalveolar unit, elucidated the differential stress-strain behavior in the PDL and revealed distinct deformation patterns in the alveolar bone and tooth structure. Stress analysis indicated that the highest von Mises stress values were observed in the inward and outward directions, particularly when force vectors were aligned with the center of resistance of the tooth. A-NiTi produced maximum PDL stress values nearing 0.038 MPa during inward displacement, while M-NiTi demonstrated a peak of approximately 0.028 MPa under the same conditions. This trend was consistent across all displacements, with A-NiTi invariably resulting in greater stress deposition in the PDL compared to M-NiTi.

In the extrusive and intrusive movements, stress levels were comparatively lower. For A-NiTi, von Mises stress ranged from 0.015 MPa to 0.027 MPa, while M-NiTi recorded slightly attenuated values between 0.012 MPa and 0.022 MPa. Notably, the PDL displayed a more uniform stress distribution in vertical displacements than in labiolingual or

combined vector movements, suggesting a more predictable biomechanical response in such clinical scenarios.

Rotational and angular movements induced the lowest stress responses in the PDL for both wire types. The values recorded were substantially reduced, with peak stresses not exceeding 0.015 MPa in A-NiTi and 0.010 MPa in M-NiTi. Correspondingly, these displacements also generated the least strain within the PDL, reaffirming their biomechanical mildness in terms of tissue loading.

The highest strain values were observed during extrusive and inward displacements, particularly with the A-NiTi wire. Inward-directed forces from A-NiTi induced strain levels approaching 10.2%, whereas M-NiTi resulted in peak strain values around 7.6% for the same direction and magnitude. The extrusive forces yielded strain magnitudes between 6% and 9% in A-NiTi and between 4.5% and 7.2% in M-NiTi. These strain values are considered biologically relevant, as they remain within the optimal loading range for inducing orthodontic tooth movement without pathological compression or ischemia in the ligament.

Tooth and bone deformation analyses revealed a consistent trend: A-NiTi generated higher displacement magnitudes in both tooth and alveolar bone compared to M-NiTi across all directions. Maximum deformation occurred in labiolingual movements, where tooth displacement exceeded 0.18 mm in A-NiTi models at 2 mm wire deflection, whereas M-NiTi models recorded displacements under 0.15 mm. Similar proportional differences were observed in bone deformation **(Table 4)**. The lowest deformation values occurred during rotational and angular movements, further confirming their minimal biomechanical impact.

Table 4. Tooth and Bone Deformation at 2 mm Displacement

Direction	Wire Type	Tooth Deformation (mm)	Bone Deformation (mm)
Extrusive	A-NiTi	0.12	0.07
Extrusive	M-NiTi	0.09	0.05
Inward	A-NiTi	0.18	0.11
Inward	M-NiTi	0.14	0.09
Outward	A-NiTi	0.17	0.10
Outward	M-NiTi	0.13	0.08
Rotational	A-NiTi	0.06	0.03
Rotational	M-NiTi	0.05	0.02

In multi-vectorial displacement simulations, involving combined directional forces (e.g., extrusive with rotational), stress accumulation in the PDL and deformation values increased multiplicatively. A-NiTi continued to produce more pronounced effects, with multi-directional displacements generating composite stress peaks that were approximately 1.5 to 2 times higher than those recorded during uniaxial loading. Comparative strain and stress effects of A-NiTi and M-NiTi under multi-directional forces are illustrated in **Figure 3**.

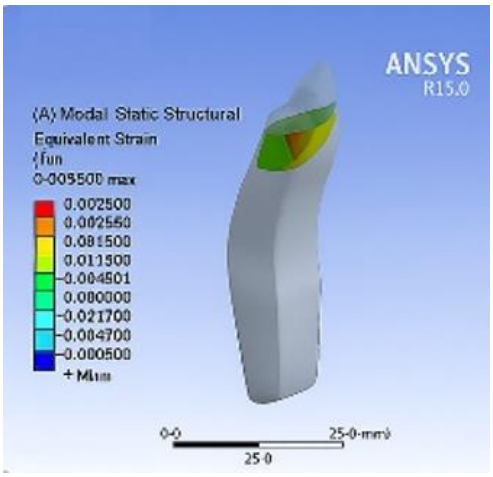

a)

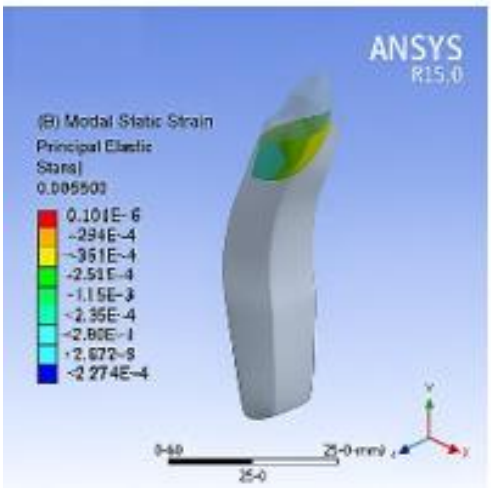

b)

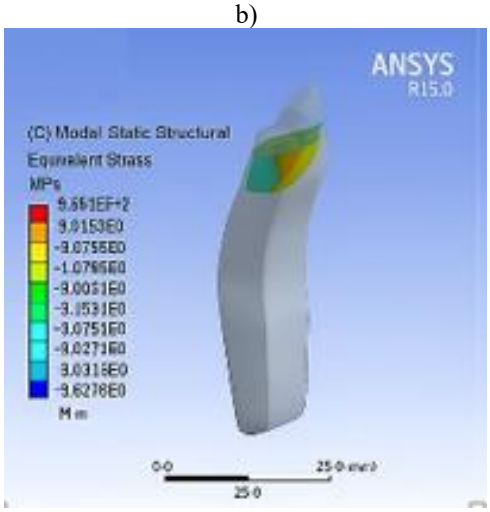

c)

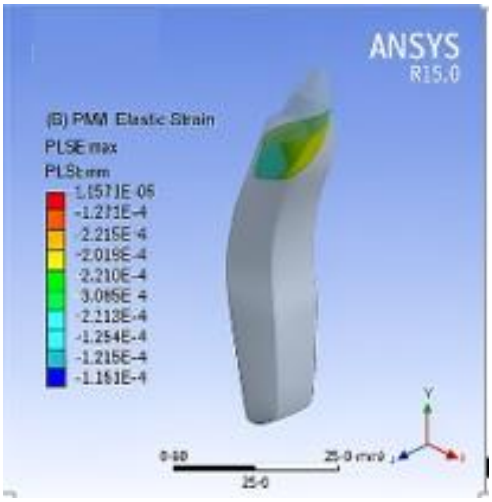

d)

Figure 3. Comparison of Principal Strain and Stress Distribution Using A-NiTi and M-NiTi Arch wires. This figure illustrates principal strain and von Mises stress distributions in the periodontal ligament (PDL) under complex displacement scenarios using A-NiTi and M-NiTi wires. The upper panels (A, B) show elastic strain concentrations in A-NiTi simulations with four-directional forces. Lower panels (C, D) show equivalent stress maps in M-NiTi under intrusive-inward and inward-outward angular displacements. The color scale ranges from blue (minimal) to red (maximum), indicating the intensity of mechanical stimuli transferred to the PDL. The comparison demonstrates the diffuse, biologically favorable stress distribution of M-NiTi relative to the concentrated effects observed with A-NiTi.

M-NiTi, although less potent in magnitude, exhibited more diffuse and evenly distributed stress patterns, indicating a potentially more favorable biological response under complex force systems.

In summary, A-NiTi wires were shown to deliver consistently higher forces and induce greater mechanical stimuli within the PDL, tooth, and surrounding bone. M-NiTi, while producing lighter forces, offered a more uniform stress distribution and lower strain values, suggesting suitability for initial alignment phases or in patients with compromised periodontal support. The directionality of displacement significantly influenced the mechanical response, with inward and outward movements generating the highest stress, strain, and deformation, followed by extrusive and intrusive, and lastly by angular and rotational movements. These findings offer a comprehensive biomechanical profile of two commonly employed NiTi arch wires, providing valuable insights for optimizing wire selection based on the desired therapeutic outcome.

The present study employed a three-dimensional finite element model (FEM) to evaluate and compare the mechanical behavior of austenitic (A-NiTi) and martensitic (M-NiTi) nickel-titanium arch wires under controlled displacements, with a focus on the resultant force magnitudes, periodontal ligament (PDL) stress-strain distribution, and dentoalveolar deformation. The findings reinforce the foundational role of wire composition and mechanical phase behavior in orthodontic biomechanics and underscore the necessity of tailoring wire selection to the intended clinical application. These results are best interpreted in light of the current literature on NiTi biomechanics and finite element modeling.

One of the primary insights emerging from this investigation is the clear difference in force magnitudes delivered by A-NiTi and M-NiTi wires under equivalent deflection conditions. A-NiTi wires consistently generated higher forces across all displacement directions, reflecting their superelastic properties and elevated plateau stress range. This finding is consistent with prior experimental observations by Kapila *et al*. who reported that superelastic NiTi alloys exhibit high spring back and sustained activation forces over extended ranges of deflection compared to heat-activated variants, which engage primarily within temperature-dependent stress thresholds [30].

The implications of this force differential extend into the clinical context. The elevated forces associated with A-NiTi may prove advantageous during early alignment phases involving significant deflections, where efficiency in overcoming severe crowding is desired. However, this advantage must be balanced against the biological tolerance of the PDL and surrounding alveolar structures. As McGuinness *et al*. demonstrated through three-dimensional finite element modeling, stress concentrations exceeding 0.025 N/mm² in the cervical and apical PDL regions could predispose to adverse responses, including root resorption or hyalinization [31]. In the present study, A-NiTi wires reached or slightly exceeded this stress threshold during inward and outward displacement scenarios, warranting caution during their prolonged use in highly displaced dentitions [32-34].

M-NiTi wires, in contrast, yielded lower stress values and strain amplitudes, suggesting a more biologically favorable force profile. This aligns with the findings of Yang Y *et al*. who showed that lower force systems, when combined with appropriate moment-to-force (M/F) ratios, can achieve efficient tooth translation while minimizing localized PDL compression [35]. Furthermore, M-NiTi wires are thermally activated and exhibit a broader transformation temperature range (TTR), which renders them less sensitive to mechanical fluctuations during insertion. Their gradual activation within the oral cavity ensures a gentler force application, a quality particularly beneficial for patients with compromised periodontal support or low pain thresholds.

The directional dependency of stress distribution observed in this study reinforces the complexity of orthodontic force systems and their interaction with anatomical geometry. Inward and outward displacements produced the highest stress and strain values in the PDL. This finding corresponds

with earlier simulations by Tanne *et al*. and Raghuveer H *et al*. who observed that labiolingual forces induced significantly higher stress concentrations in the cervical third of the PDL compared to vertical or rotational forces [36, 37]. Such directional sensitivity suggests that orthodontic tooth movement cannot be generalized across all axes and that force vector orientation plays a crucial role in determining biological response.

Rotational and angular displacements, although producing the least force, also induced minimal deformation and stress, consistent with observations by Yettram *et al*. who reported that off-axis movements, due to their limited contact area and indirect force propagation, typically result in diffuse and low-magnitude stress fields [38]. These findings imply that while A-NiTi may be appropriate for rapid initial alignment, M-NiTi could be the wire of choice when aiming to achieve delicate movements such as rotation or torque control, minimizing the risk of overloading.

It is notable that finite element analysis, as a modeling approach, allowed for high-resolution examination of stress fields within highly complex geometries such as the root-PDL-bone interface. Several prior authors have highlighted FEM's capacity to provide clinically relevant approximations of force transmission and tissue response. Katta M *et al*. noted that FEM simulations, when appropriately parameterized, reliably mirror in vivo stress-strain responses, especially when derived from patient-specific computed tomography data [39]. In this study, the use of high-fidelity anatomical models derived from CBCT scans added validity to the simulated responses and reinforced the applicability of these findings in clinical orthodontics.

While the absolute stress values differ between studies due to variation in material property assignment and boundary conditions, the relative patterns observed in this investigation mirror those in the broader literature. For example, Toms *et al*. demonstrated through cadaveric testing and FEM modeling that nonlinear PDL behavior significantly impacts stress accumulation, particularly at the apical and cervical margins [40]. The current study also observed stress peaks at these sites, particularly under inward and outward displacement forces with A-NiTi wires.

From a biomechanical standpoint, the differential stress response is not merely a product of the material properties of the wires but also of the complex interaction between the bracket slot geometry, friction coefficients, and the elastic response of adjacent tissues. Cattaneo *et al*. emphasized that finite element simulations must incorporate realistic PDL modeling and anisotropic bone behavior to predict clinical outcomes faithfully. Although the current model employed isotropic material definitions, the trends observed are nonetheless consistent with more advanced simulations that incorporate heterogeneity and nonlinearity.

Clinically, the strain thresholds identified in this study are of particular interest. The maximum PDL strains recorded, approaching 10% in some A-NiTi inward displacement simulations, reside near the upper boundary of physiological strain tolerance. Prolonged exposure to such magnitudes could lead to ischemia and sterile necrosis, as previously suggested by Attik e *et al*., who showed that intrusive and labial forces correlated strongly with increased risk of root resorption in maxillary incisors [41]. This underscores the necessity of time-modulated force application, and perhaps the intermittent use of superelastic wires in high-stress displacement cases.

Furthermore, the finding that combined (multi-vectorial) displacements amplified stress synergistically is in agreement with findings from Zhong *et al*. who demonstrated that compounded force systems generate non-linear increases in PDL load, often exceeding the sum of individual vector components [42]. In practice, this means that clinicians should anticipate and manage load interactions in crowded arches where simultaneous labiolingual and vertical correction is required.

Finally, this study affirms the broader clinical observation that M-NiTi wires may serve as a more biologically adaptive choice during early stages of orthodontic treatment. Their low continuous force delivery, combined with enhanced patient comfort and favorable stress distribution, makes them particularly suitable for initiating alignment in cases involving fragile periodontal conditions or low anchorage tolerance. On the other hand, A-NiTi wires, though capable of producing more rapid displacement due to higher force levels, must be employed judiciously, with regular monitoring to mitigate potential risks such as root resorption, as well as patient-reported discomfort or pulp sensitivity.

In summary, the present FEM-based analysis contributes valuable biomechanical insight to the comparative evaluation of A-NiTi and M-NiTi arch wires. The evidence supports a phase-specific approach to wire selection that considers not only the magnitude and direction of displacement but also the physiological tolerance of the supporting structures .

As Cattaneo *et al*. aptly observed, patient-specific modeling remains the future of precision orthodontics, wherein FEM tools may increasingly guide individualized treatment strategies. Future studies incorporating time-dependent bone remodeling algorithms and nonlinear viscoelastic modeling of the PDL will further refine our understanding of force-biologic response relationships in orthodontic therapy.

Conclusion

This three-dimensional finite element analysis underscores the critical influence of arch wire composition on the biomechanics of orthodontic tooth movement. Austenitic NiTi (A-NiTi) wires exhibited higher force output and

induced greater stress and strain within the periodontal ligament and dentoalveolar complex, particularly during labiolingual displacements. In contrast, Martensitic NiTi (M-NiTi) wires generated lighter, more biologically favorable forces with more uniform stress distribution, suggesting their appropriateness in early or sensitive treatment phases.

The direction of displacement emerged as a decisive factor in biomechanical response, with inward and outward movements producing the most pronounced mechanical effects, irrespective of wire type. These findings support a strategic, patient-specific approach to wire selection, emphasizing the need to balance mechanical efficiency with biological tolerance. By integrating realistic anatomical modeling with advanced simulation, this study contributes to the optimization of force systems in orthodontics. Future research incorporating time-dependent remodeling and viscoelastic PDL properties will be essential to enhance predictive precision and treatment individualization.

Acknowledgments: None

Conflict of interest: None

Financial support: None

Ethics statement: Ethical approval for this study was obtained from the Institutional Ethics Committee of Yenepoya (Deemed to be University), Mangalore, Karnataka, India (YUEC 294/31/12/2014)

References

1. Li Y, Jacox LA, Little SH, Ko CC. Orthodontic tooth movement: The biology and clinical implications. Kaohsiung J Med Sci. 2018;34(4):207-14. doi:10.1016/j.kjms.2018.01.007
2. Abdelrahman RSh, Al-Nimri KS, Al Maaitah EF. Pain experience during initial alignment with three types of nickel-titanium archwires: A prospective clinical trial. Angle Orthod. 2015;85(6):1021-6. doi:10.2319/071614-498.1
3. Azizi F, Extiari A, Imani MM. Tooth alignment and pain experience with A-NiTi versus Cu-NiTi: A randomized clinical trial. BMC Oral Health. 2021;21:431. doi:10.1186/s12903-021-01789-5
4. Maroof M, Sujithra R, Tewari RP. Superelastic and shape memory equi-atomic nickel-titanium (Ni-Ti) alloy in dentistry: A systematic review. Mater Today Commun. 2022;33:104352. doi:10.1016/j.mtcomm.2022.104352
5. Uysal I, Yilmaz B, Atilla AO, Evis Z. Nickel-titanium alloys as orthodontic archwires: A narrative review. Eng Sci Technol Int J. 2022;36:101277. doi:10.1016/j.jestch.2022.101277
6. Sofar MK, Rafeeq RA. Evaluation of mechanical properties of NiTi and CuNiTi archwires in as-received and artificially aged conditions. J Res Med Dent Sci. 2021;9(2):73-9. https://www.jrmds.in/articles/evaluation-of-mechanical-properties-of-niti-and-cuniti-archwires-in-as-received-and-after-artificial-aging.pdf
7. Cattaneo PM, Cornelis MA. Orthodontic tooth movement studied by finite element analysis: An update. What can we learn from these simulations? Curr Osteoporos Rep. 2021;19(2):175-81. doi:10.1007/s11914-021-00664-0
8. Cattaneo PM, Dalstra M, Melsen B. The finite element method: A tool to study orthodontic tooth movement. J Dent Res. 2005;84(5):428-33. doi:10.1177/154405910508400506
9. Gandhi A, Singh D, Fatima K, Tripathi T, Rai P. Finite element analysis—A biomechanical tool in orthodontics. IP Indian J Orthod Dentofacial Res. 2024;10(1):11-5. doi:10.18231/j.ijodr.2024.003
10. Jain AK, Savana K, Singh S, Brajendu, Roy S, Priya P. Biomechanical evaluation of different orthodontic archwire materials and their effect on tooth movement efficiency. J Pharm Bioallied Sci. 2024;16(Suppl 4):S3358-60. doi:10.4103/jpbs.jpbs_836_24
11. Knop L, Gandini LG Jr, Shintcovsk RL, Gandini MREAS. Scientific use of the finite element method in orthodontics. Dental Press J Orthod. 2015;20(2):119-25. doi:10.1590/2176-9451.20.2.119-125.sar
12. Varoneckaitė M, Jasinskaitė K, Varoneckas A, Vasiliauskas A, Leketas M. Comparing root resorption in fixed vs. clear aligner orthodontics: A radiographic study. Asian J Periodontics Orthod. 2024;4:34-41. doi:10.51847/fl7oRw6Djo
13. Zhou J, Bazar KAO, Bin W. Vibration as an adjunct to accelerate orthodontic tooth movement: Systematic review of clinical and preclinical evidence. Asian J Periodontics Orthod. 2024;4:60-74. doi:10.51847/ZWrGaDObiC
14. Safa AS, Farkas ER. Physicians' implicit attitudes toward obese and mentally ill patients: Effects of specialty and experience. Asian J Ethics Health Med. 2024;4:58-67. doi:10.51847/7T31yxI8jU
15. Leadbeatter D, Tjaya KC. Human rights and bioethical principles in correctional settings: A systematic review of the evidence. Asian J Ethics Health Med. 2024;4:97-106. doi:10.51847/wSNBedLrGt
16. Sugimori T, Yamaguchi M, Kikuta J, Shimizu M, Negishi S. The biomechanical and cellular response to micro-perforations in orthodontic therapy. Asian J Periodontics Orthod. 2022;2:1-15. doi:10.51847/Z9adSJ59rj
17. Dipalma G, Inchingolo AD, Fiore A, Balestriere L, Nardelli P, Casamassima L, et al. Comparative effects of fixed and clear aligner therapy on oral microbiome dynamics. Asian J Periodontics Orthod. 2022;2:33-41. doi:10.51847/mK28wdKCIX
18. Samaranayake L, Tuygunov N, Schwendicke F, Osathanon T, Khurshid Z, Boymuradov SA, et al. Artificial intelligence in prosthodontics: Transforming diagnosis and treatment planning. Asian J Periodontics Orthod. 2024;4:9-18. doi:10.51847/nNyZ6VD1da

19. Prada AM, Cicalău GIP, Ciavoi G. Resin infiltration for white-spot lesion management after orthodontic treatment. Asian J Periodontics Orthod. 2024;4:19-23. doi:10.51847/ZTuGEanCSV
20. Iryna L, Dmytro L, Kseniia M, Olena B, Alina S, Dmytro M. Rational approach to pharmacotherapy in respiratory diseases during the COVID-19 pandemic. J Med Sci Interdiscip Res. 2022;2(1):9-14. doi:10.51847/paRajRCk5I
21. Palaiodimos L, Ali R, Teo HO, Parthasarathy S, Karamanis D, Chamorro-Pareja N, et al. Exploring the role of CRP analysis and obesity in the disparities of COVID-19 outcomes. J Med Sci Interdiscip Res. 2022;2(1):1-8. doi:10.51847/GnA3T0sCP1
22. ElKenawy HA, Alsaeed MI, Najmi AA, Al Ghalbi AN, Daiwali IG, Alshuhay AH, et al. Role of computed tomography in the staging and management of colorectal cancer: A clinical assessment. Arch Int J Cancer Allied Sci. 2023;3(1):10-5. doi:10.51847/bXYhJyLnSd
23. Tsvetkova D, Vezenkov L, Ivanov T, Danalev D, Kostadinova I. Evaluation of cytotoxic effects induced by galantamine-linked peptide esters on HeLa cell line via MTT assay. Arch Int J Cancer Allied Sci. 2023;3(1):1-9. doi:10.51847/5DEuPlWlDX
24. Kim S, Bae H, Kim H. A diagnostic and therapeutic dilemma: Giant multifocal retroperitoneal dedifferentiated liposarcoma with dual heterologous components. Arch Int J Cancer Allied Sci. 2024;4(2):1-5. doi:10.51847/5JnC3jAkZz
25. Huang L, Li H, Chen J, Jiang J, Zhang W, Liu T. Challenges in the management of delayed port-site metastasis in gallbladder adenocarcinoma: A case study and review of the literature. Arch Int J Cancer Allied Sci. 2024;4(2):6-10. doi:10.51847/sYmcCYwIR1
26. Lee MJ, Ferreira J. COVID-19 and children as an afterthought: Establishing an ethical framework for pandemic policy that includes children. Asian J Ethics Health Med. 2024;4:1-19. doi:10.51847/haLKYCQorD
27. Negreiros AB, Ory MG. Navigating uncertain outcomes: Returning genomic results in children with developmental delays. Asian J Ethics Health Med. 2024;4:20-7. doi:10.51847/grOfZd8oyo
28. Abdelkader H, Bergeron S. Exploring professionals' views on the ethical considerations of clinically provided safer injection education for people who inject drugs. Asian J Ethics Health Med. 2022;2:1-9. doi:10.51847/4rEkDE06Lw
29. Masamura N, Nishiyama T, Sugimori T. Navigating incidental findings in genomic research: Professional attitudes and practices. Asian J Ethics Health Med. 2022;2:36-43. doi:10.51847/bIf5NmI7Ju
30. Kapila S, Sachdeva R. Mechanical properties and clinical applications of orthodontic wires. Am J Orthod Dentofacial Orthop. 1989;96(2):100-9. doi:10.1016/0889-5406(89)90251-5
31. McGuinness NJ, Wilson AN, Jones ML, Middleton J. A stress analysis of the periodontal ligament under various orthodontic loadings. Eur J Orthod. 1991;13(3):231-42. doi:10.1093/ejo/13.3.231
32. Stanbouly D, Radley B, Steinberg B, Ascherman JA, Zimmer TS. Epilepsy in individuals with craniosynostosis: A comprehensive review. Interdiscip Res Med Sci Spec. 2022;2(1):1-7. doi:10.51847/g1TR0ZrWVL
33. Florina MG, Mariana G, Csaba N, Gratiela VL. Exploring the interconnection between diet, microbiome, and human health: A systematic review. Interdiscip Res Med Sci Spec. 2022;2(1):8-14. doi:10.51847/i78sbSkbZV
34. Delcea C, Rad D, Gyorgy M, Runcan R, Breaz A, Gavrilă-Ardelean M, et al. Exploring Romanian resilience: A network analysis of coping mechanisms during the COVID-19 pandemic. Int J Soc Psychol Asp Healthc. 2023;3:13-20. doi:10.51847/HgPIOyOclr
35. Yang Y, Tang W. Analysis of the influence of bracket and force system directions on moment-to-force ratio using the finite element method. Eurasip J Wirel Commun Netw. 2018;2018:1-10. doi:10.1186/s13638-018-1187-1
36. Raghuveer H, Hemanth M, Rani M, Hegde C, Vedavathi B, Chaithra D. Stress induced in the periodontal ligament during extrusion and rotation movements: A finite element method study. J Contemp Dent Pract. 2015;16(9):740-3. doi:10.5005/jp-journals-10024-1750
37. Tanne K, Yoshida S, Kawata T, Sasaki A, Knox J, Jones ML. Evaluation of the biomechanical response of the tooth and periodontium to orthodontic forces in adolescent and adult subjects. Br J Orthod. 1998;25(2):109-15. doi:10.1093/ortho/25.2.109
38. Yettram AL, Wright KW, Pickard HM. Finite element stress analysis of the crowns of normal and restored teeth. J Dent Res. 1976;55(6):1004-11. doi:10.1177/00220345760550060201
39. Katta M, Petrescu SM, Dragomir LP, Popescu MR, Georgescu RV, Țuculină MJ, et al. Using the finite element method to determine the odonto-periodontal stress for a patient with Angle Class II Division 1 malocclusion. Diagnostics (Basel). 2023;13(9):1567. doi:10.3390/diagnostics13091567
40. Toms SR, Eberhardt AW. A nonlinear finite element analysis of the periodontal ligament under orthodontic tooth loading. Am J Orthod Dentofacial Orthop. 2003;123(6):657-65. doi:10.1016/S0889-5406(03)00164-1
41. Zhong J, Shibata Y, Wu C, Watanabe C, Chen J, Zheng K, et al. Functional non-uniformity of periodontal ligaments tunes mechanobiological stimuli across tissue interfaces. Acta Biomater. 2023;170:240-9. doi:10.1016/j.actbio.2023.08.047
42. Atik E, Gorucu-Coskuner H, Akarsu-Guven B, Taner T. Evaluation of changes in the maxillary alveolar bone after incisor intrusion. Korean J Orthod. 2018;48(6):367. doi:10.4041/kjod.2018.48.6.367